

Fault Current Limiting and Magnetizing Characteristics of the Autotransformer Type SFCL

Min Ki Park and Sung Hun Lim[†]

Department of Electrical Engineering, Soongsil University, Seoul 06978, Korea

Received January 16, 2017; Accepted January 16, 2017

In designing the autotransformer type superconducting fault-current limiter (SFCL), one must consider that the iron core can be saturated for the SFCL to have effective fault-current limiting operation. In this paper, to examine the saturation of the iron core comprising SFCL during the fault period, the linkage flux and the magnetizing current of the SFCL were derived from the electrical equivalent circuit with the nonlinear exciting branch. By analysis on the linkage flux versus the magnetizing current of the autotransformer type SFCL, calculated from the short-circuit tests, the design condition for the suppression of the iron core's saturation was discussed.

Keywords: Autotransformer superconducting fault current limiter (SFCL), Saturation of iron core, Fault current limiting operation, Magnetizing current

1. INTRODUCTION

Since the superconducting fault current limiters (SFCLs) have been considered to an effective method for reducing fault currents, various types of SFCLs have been developed. Among the developed SFCLs, the transformer type SFCL, such as the hybrid and flux-lock types, has the merit that it can be adjusted by the turn ratio between two coils. However, the SFCL must be designed in terms of the saturation of the iron core, which is the essential component of the transformer type SFCL [1-6]. The autotransformer type SFCL, which is analyzed in this paper, has a simpler structure than other types of SFCLs and will probably continue to be studied in order to improve its fault current limiting operation. However, more analysis on the saturation of the iron core comprising the autotransformer type SFCL, like the previous transformer type SFCL that also used an iron core, is required.

In this paper, the electrical equivalent circuit of the autotransformer type SFCL, including the magnetizing branch, was drawn, and the magnetizing current, which is related to the saturation of the iron core, was derived. As one design parameter to

affect the saturation of the iron core comprising the autotransformer type SFCL, the tap ratio of the SFCL was considered. With the linkage flux and the magnetizing current, which was calculated from its equivalent circuit, the fault current limiting and the magnetizing characteristics of the SFCL were analyzed.

2. STRUCTURE AND EQUIVALENT CIRCUIT OF SFCL

2.1 Operational principle

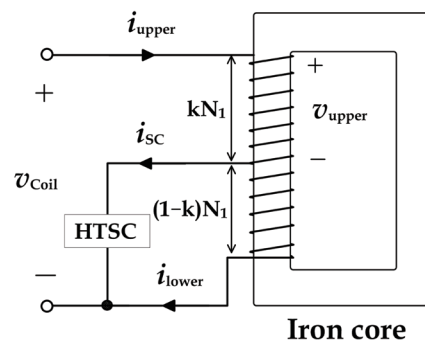


Fig. 1. Configuration of the autotransformer type SFCL.

[†] Author to whom all correspondence should be addressed:
E-mail: superish73@ssu.ac.kr

Figure 1 shows a configuration of the autotransformer type SFCL, which is made of the coil with a tap wound on the iron core and a high-TC superconducting (HTSC) element; k , representing the tap location on the coil, has a value between 0 and 1. With the change of the tap location, the induced voltage in the HTSC element during its quench generation is thought to be adjusted.

The basic operational principle of the SFCL is the same as that of the transformer type SFCL, such as the hybrid and flux-lock types, as reported in [4-6].

2.2 Equivalent circuit

The equivalent circuit of the autotransformer-type SFCL for the analysis of its magnetizing characteristics consists of the magnetization inductance (L_m) and the resistance (R_c) of the iron core loss, as shown in Fig. 2.

R_{upper} , R_{lower} and L_{upper} , L_{lower} represent the resistances and the leakage inductances of the upper and lower parts of the coil,

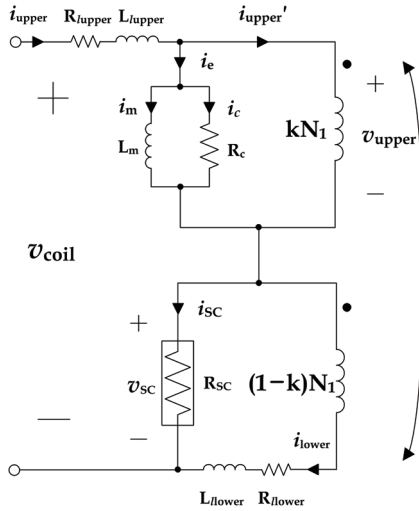


Fig. 2. Electrical equivalent circuit of the autotransformer type SFCL.

respectively. Since i_{upper} has a relation to i_{lower} as expressed in Eq. (1), the magnetizing current (i_m) can be calculated as Eq. (2) if the iron core loss is lower. The linkage flux generated within the iron core (λ_m) can be calculated by integrating the voltage across the upper part of the coil (v_{upper}) assuming that the leakage flux and the resistance of the coil is ignored.

$$i_{\text{upper}}' = \frac{1-k}{k} i_{\text{lower}} \tag{1}$$

$$i_m = i_{\text{upper}} - i_{\text{upper}}' \tag{2}$$

As seen in Eqs. (1) and (2), the linkage flux and the magnetizing current of the iron core depend on the tap location. With the linkage flux and the magnetizing current, the magnetizing curves of the iron core of the SFCL can be obtained.

2.3 Experimental preparation

The design parameters for the SFCL are listed in Table 1. This SFCL consists of an HTSC element, one coil wound on the iron core, and a tap changer to change the tap location. As the HTSC element connected with the tap of the coil, a $Y_1Ba_2Cu_3O_{7-x}$ (YBCO) thin film was used. The schematic test circuit to apply the short-circuit current to the SFCL, as shown in Fig. 3, consists of a 60 Hz ac

power supply, a series resistance, a load resistance, and the SFCL. After SW₁ was closed, SW₂ at 0° of the source voltage was closed and was again opened after five cycles. The voltage and the current data were measured with the current transformer and the potential transformer.

Table 1. Design parameters for the fabricated SFCL.

Iron core (silicon steel)	Value	Unit
Outer horizontal length	235	mm
Outer vertical length	250	mm
Inner horizontal length	137	mm
Inner vertical length	155	mm
Thickness	132	mm
Coil with tap changer	Value	Unit
N_1	84	Turns
Tap location (k)	0.75, 0.60	
HTSC elements	Value	Unit
Fabrication type	Thin film	
Critical temperature	87	K
Critical current	19	A

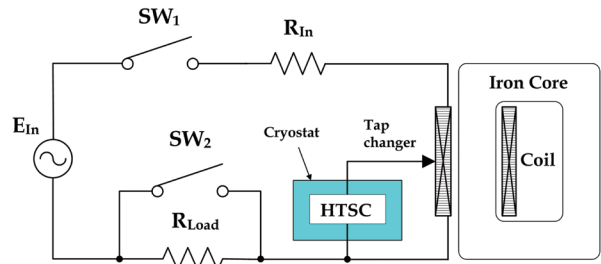


Fig. 3. Schematic test circuit to apply the short-circuit current to the SFCL.

3. RESULTS AND DISCUSSIONS

Figures 4 and 5 show the fault current limiting characteristics of an SFCL when k is 0.75. The directions of the currents flowing across the lower part of the coil and the HTSC element (i_{lower} , i_{SC}), as compared in Fig. 4(b), are opposed before the fault occurs. The magnetizing current (i_m), as shown in Fig. 4(a), can be derived from the currents at the upper and the lower parts of the coil (i_{upper} , i_{lower})

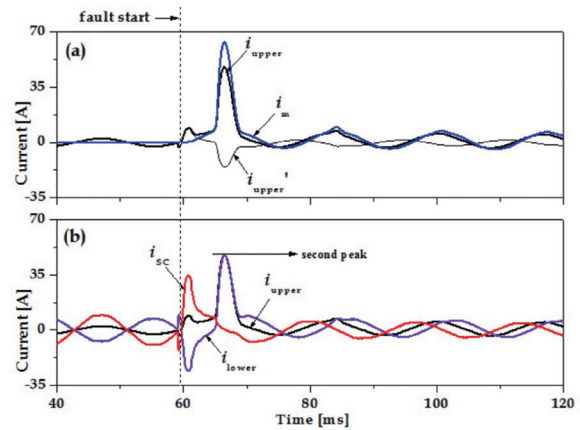


Fig. 4. Fault current limiting characteristics of the SFCL when k is 0.75. (a) Current of upper part (i_{upper}), current of lower part viewed from the upper part (i_{upper}) and magnetizing current (i_m). (b) Currents of upper and lower parts (i_{upper} , i_{lower}), current of HTSC element (i_{SC}).

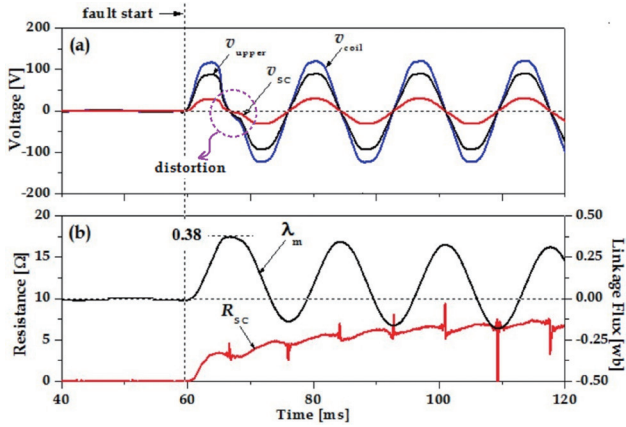


Fig. 5. Fault current limiting characteristics of the SFCL when k is 0.75. (a) Voltage of upper part of coil (v_{upper}), voltage of coil (v_{coil}), and voltage across HTSC element (v_{sc}). (b) Linkage flux (λ_m) and resistance of HTSC element (R_{sc}).

using Eqs. (1) and (2).

The magnetizing current (i_m), which is at zero value before the fault occurs, sharply increases and makes larger distortions in the voltage waveforms (v_{upper} , v_{coil} , v_{sc}) directly after the fault occurs as indicated with arrow in Fig. 5(a).

The sharply increased magnetizing current at the initial fault time causes the second peak in the current of the upper part of the coil (i_{upper}), as seen in Fig. 4(b), in spite of the resistance generated in the HTSC element (R_{sc}), as displayed in Fig. 5(b).

From the analysis, the sharply increased magnetizing current, which resulted from the saturation of the iron core in the SFCL, deteriorates the fault current limiting of the SFCL.

The voltages across the coil and the upper part (v_{coil} , v_{upper}), which are almost zero before the fault, as seen in Fig. 5(a), are generated proportionally to the number of the coil's turns after the fault occurs. The linkage flux (λ_m) in Fig. 5(b), which can be calculated by integrating the induced voltage in the upper part of the coil (v_{upper}), increases up from almost zero immediately after the fault starts and decreases gradually from a maximum value of 0.38 [wb] as time passes.

To investigate the magnetizing and fault current limiting characteristics of the SFCL caused by the induced voltage in the

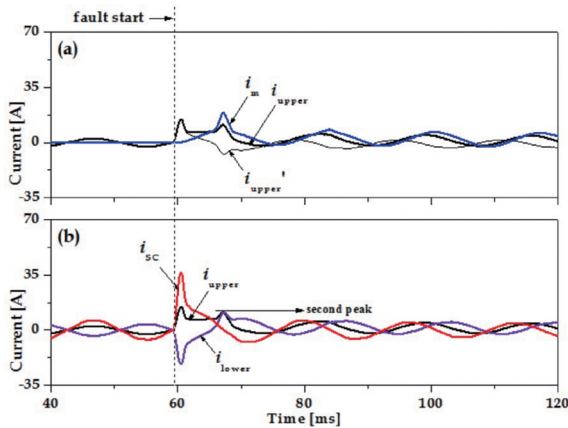


Fig. 6. Fault current limiting characteristics of the SFCL when k is 0.60. (a) Current of upper part (i_{upper}), current of lower part viewed from the upper part (i_{upper}), and magnetizing current (i_m). (b) Currents of upper and lower parts (i_{upper} , i_{lower}), current of HTSC element (i_{sc}).

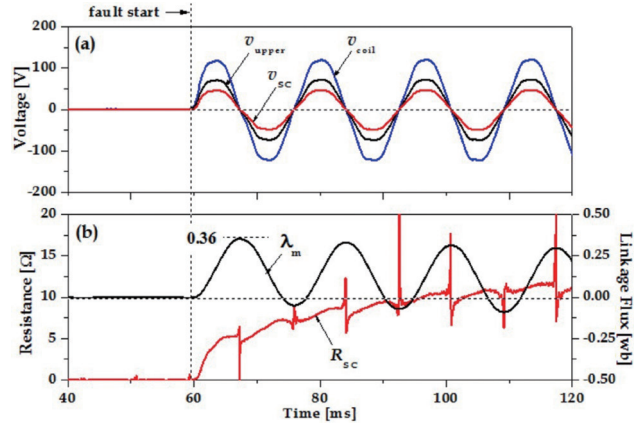


Fig. 7. Fault current limiting characteristics of the SFCL when k is 0.60. (a) Voltage of upper part of coil (v_{upper}), voltage of coil (v_{coil}), and voltage across the HTSC element (v_{sc}). (b) Linkage flux (λ_m) and resistance of HTSC element (R_{sc}).

HTSC element during its quench generation after the fault happens, the tap location was changed from 0.75 to 0.60.

Figures 6 and 7 show the fault current limiting characteristics of the SFCL when k is 0.60. The induced voltage in the HTSC element (v_{sc}), as seen in Fig. 7(a), increases more than when k is 0.75, which is also compared with the resistance curves of the HTSC element from Figs. 5(b) and 7(b). The increased induced voltage of the HTSC element (v_{sc}), when k is 0.60, lowers the magnetizing current (i_m) and the second peak in the current of the upper part of the coil (i_{upper}) and contributes to the decreased distortion in the voltage waveforms (v_{upper} , v_{coil} , v_{sc}) as seen in Fig. 7(a).

As analyzed above, the increased induced voltage (v_{sc}) in the HTSC element during the fault period suppresses the iron core's saturation of the SFCL, which helps improve the fault current

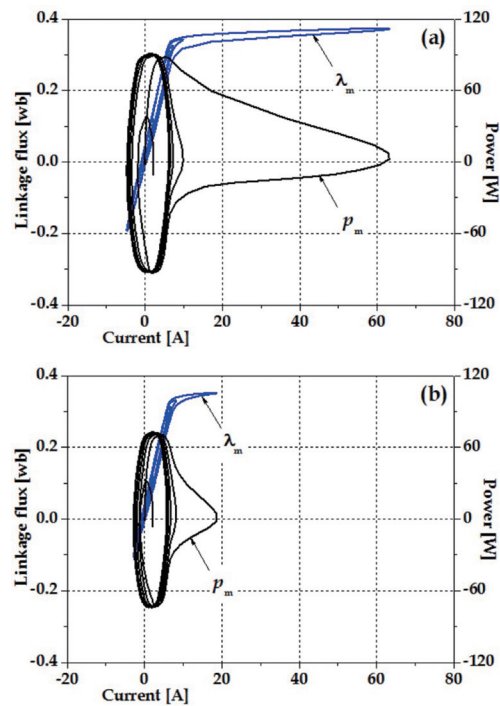


Fig. 8. Variation of linkage flux's operational range (λ) and magnetizing power (p_m) dependent on magnetization current (i_m) during the fault period in the SFCL. (a) When k is 0.75. (b) When k is 0.60.

limiting characteristics of the SFCL.

With the magnetizing current and the linkage flux obtained for the two k values of 0.75 and 0.6, the magnetizing curves of the iron core in the SFCL during the fault periods are displayed in Fig. 8. The magnetizing curves show that the linkage flux's operational range of the iron core (λ_m) with k of 0.6 recovered into the linear region after half a cycle with the small magnetizing power area (p_m), as shown in Fig. 8(b). On the other hand, the operational range of the iron core with the k of 0.75 moved into the nonlinear region during the initial fault period with the larger magnetizing power area, as compared with Fig. 8(a).

4. CONCLUSIONS

In this study, the fault-current limiting and magnetizing characteristics of the autotransformer type SFCL caused by its tap ratio, which could adjust the induced voltage in the HTSC element, were investigated by means of the measured voltages and the currents through the short-circuit tests. For the analysis of the dependence of the magnetizing characteristics of the SFCL on the induced voltage in the HTSC element, the linkage flux and the magnetizing current were derived from the electrical equivalent circuit consisting of the ideal transformer with the nonlinear magnetizing branch. For the SFCL designed with the larger induced

voltage in the HTSC element by tap changer, the saturation of the iron core of the SFCL was suppressed more than in the one designed with less induced voltage in the HTSC element.

REFERENCES

- [1] S. H. Lim, Y. S. Cho, H. S. Choi, and B. S. Han, *IEEE Trans. Appl. Supercond.*, **17**, 1807 (2007). [DOI: <https://doi.org/10.1109/TASC.2007.899246>]
- [2] S. H. Lim, *IEEE Trans. Appl. Supercond.*, **17**, 1895 (2007). [DOI: <https://doi.org/10.1109/TASC.2007.899869>]
- [3] Y. Zhao, T. K. Shah, O. Krause, and Y. Li, *IET Gener., Transmiss. Distrib.*, **10**, 548 (2016). [DOI: <https://doi.org/10.1049/iet-gtd.2015.1020>]
- [4] S. H. Lim, J. F. Moon, and J. C. Kim, *IEEE Trans. Appl. Supercond.*, **19**, 1900 (2009). [DOI: <https://doi.org/10.1109/TASC.2009.2018053>]
- [5] S. H. Lim, *Physica C*, **470**, 1631 (2010). [DOI: <https://doi.org/10.1016/j.physc.2010.05.177>]
- [6] S. H. Lim, H. J. Ahn, and C. K. Park, *IEEE Trans. Appl. Supercond.*, **24**, 5600704 (2014).
- [7] S. H. Lim, S. C. Ko, and T. H. Han, *Physica C*, **484**, 253 (2013). [DOI: <https://doi.org/10.1016/j.physc.2012.03.011>]